GPCR SIGNALING

Dynamic interactions of the 5-HT$_6$ receptor with protein partners control dendritic tree morphogenesis

Camille N. Pujol[1], Vincent Dupuy[1], Martial Séveno[2], Leonie Runtz[1,3], Joël Bockaert[1], Philippe Marin[1]*†, Séverine Chaumont-Dubel[1]*†

The serotonin (5-hydroxytrypatmine) receptor 5-HT$_6$ (5-HT$_6$R) has emerged as a promising target to alleviate the cognitive symptoms of neurodevelopmental diseases. We previously demonstrated that 5-HT$_6$R finely controls key neurodevelopmental steps, including neuronal migration and the initiation of neurite growth, through its interaction with cyclin-dependent kinase 5 (Cdk5). Here, we showed that 5-HT$_6$R recruited G protein–regulated inducer of neurite outgrowth 1 (GPRIN1) through a G$_s$-dependent mechanism. Interactions between the receptor and either Cdk5 or GPRIN1 occurred sequentially during neuronal differentiation. The 5-HT$_6$R–GPRIN1 interaction enhanced agonist-independent, receptor-stimulated cAMP production without altering the agonist-dependent response in NG108-15 neuroblastoma cells. This interaction also promoted neurite extension and branching in NG108-15 cells and primary mouse striatal neurons through a cAMP-dependent protein kinase A (PKA)–dependent mechanism. This study highlights the complex allosteric modulation of GPCRs by protein partners and demonstrates how dynamic interactions between GPCRs and their protein partners can control the different steps of highly coordinated cellular processes, such as dendritic tree morphogenesis.

INTRODUCTION

Over the last two decades, it has become evident that G protein–coupled receptors (GPCRs) do not solely recruit canonical signaling proteins, such as heterotrimeric G proteins and β-arrestins (*1*), but that they also interact with large networks of intracellular proteins that finely control their targeting to specific subcellular compartments, their trafficking in and out of the plasma membrane, and their signaling (*2*–*5*). These complexes have been extensively described for certain GPCRs by means of unbiased interactomics screens (*2*, *3*, *6*, *7*) and often include several proteins that interact with common binding sites within a given GPCR, stressing the importance of spatiotemporal regulation of the interactions of GPCRs with their protein partners in their pathophysiological functions. However, the dynamics of the associations of GPCRs with interacting proteins and their functional outcomes remain poorly characterized.

The serotonin (5-hydroxytryptamine) receptor 5-HT$_6$ (5-HT$_6$R) is a G$_s$-coupled receptor exclusively expressed in the nervous system. The highest receptor densities are found in regions involved in mnemonic functions (*8*–*12*). Consistent with this particular distribution, the 5-HT$_6$R has emerged as a promising target to alleviate the cognitive symptoms of various neurological and psychiatric disorders (*13*). 5-HT$_6$R blockade relieves deficits in a wide range of models of cognitive impairment in rodents, and preliminary clinical studies have unequivocally shown procognitive effects of several 5-HT$_6$R antagonists in humans (*14*–*17*). However, any initial hope has been tempered by the failure of phase 3 trials of the leading compound idalopirdine (Lu AE58054) used in conjunction with the acetylcholine esterase inhibitor donepezil in patients with Alzheimer's disease (*18*).

The 5-HT$_6$R is also expressed early during neuronal development, and studies have demonstrated its crucial role in both the correct migration and positioning of neurons, neurite growth, and neuronal differentiation (*19*, *20*). Further lines of evidence showed that most of the effect of the receptor on neuronal development is independent of its coupling to G$_s$, suggesting the involvement of alternative signaling mechanisms (*21*). To address this issue, genetic and proteomics strategies were used to characterize the 5-HT$_6$R interactome (*20*, *22*–*27*). These studies showed that the receptor interacts with several proteins of the mechanistic target of rapamycin (mTOR) pathway, including mTOR itself, and that 5-HT$_6$R–elicited mTOR activation in the prefrontal cortex underlies cognitive deficits in neurodevelopmental models of schizophrenia in rodents (*25*). These studies also revealed that the 5-HT$_6$R recruits cyclin-dependent kinase 5 (Cdk5), as well as several of its targets that are involved in neurite growth and synaptogenesis (*20*). The interaction between 5-HT$_6$R and Cdk5 induces the phosphorylation of the receptor by Cdk5, which promotes the initiation of neurite growth through a Cdc42-dependent pathway (*20*). Further experiments showed that the 5-HT$_6$R also controls neuronal migration through a Cdk5-dependent mechanism (*19*).

Another important feature of the 5-HT$_6$R is its high level of constitutive activity, which was established not only for recombinant receptors expressed in cell lines (*28*) but also for native receptors in cultured neurons and mouse brain (*29*). Furthermore, the receptor constitutively activates not only the canonical G$_s$ signaling pathway but also Cdk5 signaling through a mechanism dependent on receptor phosphorylation by associated Cdk5 (*20*), highlighting the potential influence of GPCR-interacting proteins (GIPs) upon GPCR constitutive activity. One of the Cdk5 substrates known to control neurodevelopmental processes identified in the 5-HT$_6$R interactome is G protein–regulated inducer of neurite outgrowth 1 (GPRIN1), which is a member of a protein family consisting of three gene products (GPRIN1 to GPRIN3) (*30*). GPRIN1 is highly abundant in the brain, binds selectively to activated G proteins, and promotes neurite extension (*30*–*32*). Several lines of evidence suggest that GPRIN1 promotes neurite growth through its direct interaction with membrane-bound receptors (*32*, *33*).

[1]Institut de Génomique Fonctionnelle, Université de Montpellier, CNRS, INSERM, Montpellier, France. [2]BioCampus Montpellier, Université de Montpellier, CNRS, INSERM, Montpellier, France. [3]Department of Psychiatry, McGill University, Douglas Hospital Research Center, Montreal, Canada.
*These authors contributed equally to this work.
†Corresponding author. Email: philippe.marin@igf.cnrs.fr (P.M.); severine.chaumont-dubel@igf.cnrs.fr (S.C.-D.)

Here, we demonstrated that 5-HT$_6$R interacted sequentially with Cdk5 and GPRIN1 during the differentiation of NG108-15 neuroblastoma cells. Functional studies showed that the interaction between the 5-HT$_6$R and GPRIN1 potentiated 5-HT$_6$R constitutive activity and promoted neurite elongation and branching in an agonist-independent, but adenosine 3′,5′-monophosphate (cAMP)–dependent, manner in both neuroblastoma cells and primary striatal neurons. Together, these findings suggest that the 5-HT$_6$R promotes neuronal differentiation through sequential engagement of different signaling pathways that depends on agonist-independent allosteric receptor activation by distinct interacting proteins.

RESULTS

The 5-HT$_6$R forms a complex with GPRIN1 in mouse brain

Using an affinity purification–mass spectrometry proteomic approach and the 5-HT$_6$R C-terminal domain as bait, we previously demonstrated the physical association of the 5-HT$_6$R with a network of proteins known to control key neurodevelopmental processes, such as the migration of neurons and neurite growth. These interaction partners include Cdk5 and some of its regulators and substrates, such as GPRIN1 (Fig. 1A). Given the developmental pattern of 5-HT$_6$R and GPRIN1 expression (*8*, *34*) and their common influence upon neuronal differentiation (*20*, *32*, *35*), we first confirmed the existence of the 5-HT$_6$R–GPRIN1 interaction in the brains of newborn mice, taking advantage of knock-in (KI) mice expressing the 5-HT$_6$R fused to green fluorescent protein (GFP; 5-HT$_6$R–GFP) (*29*). GPRIN1 coimmunoprecipitated with 5-HT$_6$R–GFP from brain protein extracts, indicating an association between the receptor and GPRIN1 (Fig. 1B). Corroborating these findings, immunohistochemistry combined with confocal microscopy showed the colocalization of the receptor and GPRIN1 in the soma of striatal (Fig. 1C) and cortical (fig. S1A) neurons from newborn 5-HT$_6$R–GFP KI mice. Consistent with previous findings that showed expression of the 5-HT$_6$R in the primary cilium (*36*–*39*), GFP immunostaining was also detected on cilia-like processes positively stained with an antibody against Arl13b (fig. S1A), a cilial marker, in both the striatum and cortex, but no colocalization between 5-HT$_6$R and GPRIN1 was found in the primary cilium. Amplifying the signal from the GFP antibody also uncovered a small population of receptors that displayed a somatodendritic localization in cultured striatal neurons from 5-HT$_6$R–GFP KI mice, but not wild-type (WT) mice. Furthermore, these somatodendritic receptors were colocalized with GPRIN1 (fig. S1B).

The 5-HT$_6$R sequentially interacts with Cdk5 and GPRIN1 in NG108-15 cells

Our interactomics screen showed that both Cdk5 and GPRIN1 interact with the 5-HT$_6$R C-terminal domain (*20*). To better characterize the dynamics of these interactions and to explore whether they occurred simultaneously or were exclusive, we performed immunoprecipitation experiments in NG108-15 cells transfected with complementary DNAs (cDNAs) encoding 5-HT$_6$R and either GPRIN1 or Cdk5. In cells coexpressing GPRIN1 and 5-HT$_6$R, we detected an interaction by immunoprecipitation 24 hours after transfection of the cells with both cDNAs, which was statistically significantly increased after 48 hours (Fig. 1D and fig. S2A). In contrast, although we observed an interaction between the receptor and Cdk5 24 hours after transfection, this was followed by dissociation of the complex 48 hours after transfection, as shown by coimmunoprecipitation experiments (Fig. 1E and fig. S2B). These findings were confirmed with bioluminescence resonance energy transfer (BRET)–based assays (Fig. 1F): A specific BRET signal was detected in NG108-15 cells coexpressing 5-HT$_6$R–yellow fluorescent protein (YFP) and Cdk5 24 hours after transfection, whereas no interaction between the two proteins was detected 48 hours after transfection. These results indicate that the receptor sequentially interacts with Cdk5 and GPRIN1 in NG108-15 cells, suggesting that the receptor's interaction partners are dynamically regulated.

Because Cdk5 phosphorylates the 5-HT$_6$R on serine 350 (Ser^{350}), we wondered whether this phosphorylation event modulated the interaction between the receptor and GPRIN1. We found that a receptor having a mutation that prevented the phosphorylation of the receptor by Cdk5 (S350A mutant) interacted to a greater extent with GPRIN1 than did the WT receptor (fig. S3A). In contrast, a mutant mimicking the phosphorylation of Ser^{350} (S350D) did not interact with GPRIN1. Similarly, overexpressing p35, a coactivator of Cdk5, to enhance Ser^{350} phosphorylation reduced the association between WT 5-HT$_6$R and GPRIN1 (fig. S3, A and B). This suggests that the 5-HT$_6$R is unable to interact with GPRIN1 when it is phosphorylated by Cdk5.

The association between GPRIN1 and the 5-HT$_6$R depends on G proteins and the conformational state of the receptor

The amount of GPRIN1 that coimmunoprecipitated with a mutant of the 5-HT$_6$R unable to activate G proteins [the triple mutant F69 L T70D D72A; (*40*)] or a mutant 5-HT$_6$R lacking the C-terminal domain (ΔCter) was statistically significantly reduced when compared with the amount of GPRIN1 that coimmunoprecipitated with the full-length, WT receptor (Fig. 1G and fig. S2C). Combining the triple mutation with the C-terminal deletion abolished the ability of the receptor to coimmunoprecipitate with GPRIN1, suggesting that both the C-terminal domain of the receptor and the ability of the receptor to activate G proteins are required for the formation of the 5-HT6R–GPRIN1 complex (Fig. 1G). To confirm the involvement of the receptor C-terminal domain in the 5-HT$_6$-R–GPRIN1 interaction, we attempted to immunoprecipitate the WT receptor and GPRIN1 from cells treated with an interfering peptide corresponding to residues 320 to 342 of the C-terminal tail of 5-HT$_6$R fused to the transduction domain of the HIV TAT protein (TAT-Ct320–342 peptide). Reminiscent of the effect of the C-terminal domain truncation, exposing cells to the TAT-Ct320–342 peptide reduced the amount of GPRIN1 that coimmunoprecipitated with the 5-HT$_6$R when compared with that in cells exposed to a control peptide (Fig. 1H and fig. S2D). Last, the amount of GPRIN1 that coimmunoprecipitated with the 5-HT$_6$R was reduced by exposing cells to the 5-HT$_6$R antagonist SB271046 (Fig. 1I and fig. S2E), which behaves as an inverse agonist with respect to receptor-operated G$_s$ signaling, suggesting that the binding of GPRIN1 to the 5-HT$_6$R is a dynamic process that depends on the conformational state of the receptor.

The interaction between GPRIN1 and the 5-HT$_6$R enhances receptor constitutive activity

We previously demonstrated that the 5-HT$_6$R exhibits constitutive activation of the G$_s$ pathway in NG108-15 neuroblastoma cells and in striatal neurons (*20*, *29*). Using the CAMYEL cAMP BRET sensor (*41*), we found that coexpressing GPRIN1 with the 5-HT$_6$R did not change basal cAMP production 24 hours after transfection of the NG108-15 cells, whereas it enhanced agonist-independent

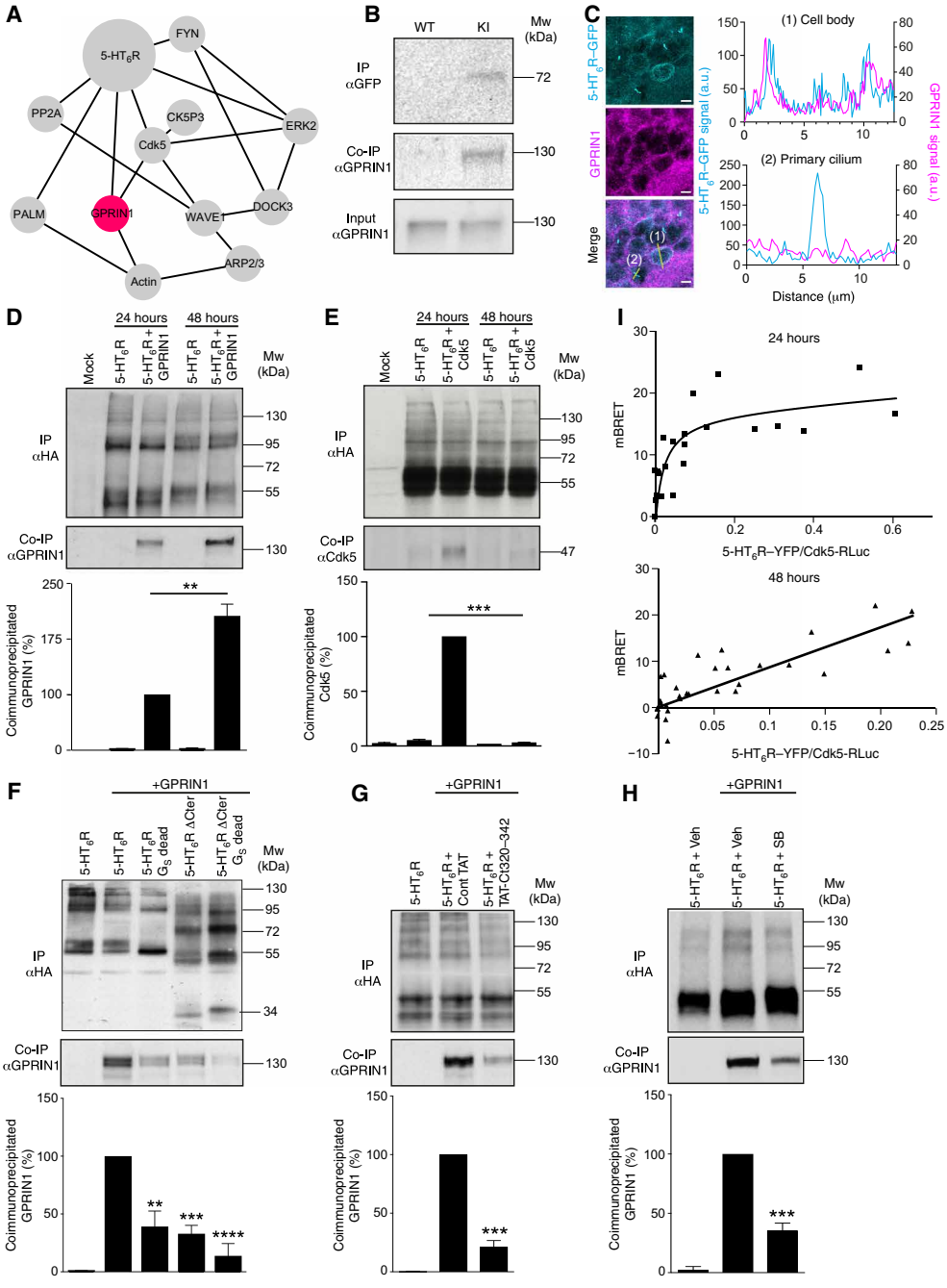

Fig. 1. Association of the 5-HT$_6$R with GPRIN1 requires both the receptor C-terminal domain and G_s protein. (**A**) A simple interaction file was designed and imported in Cytoscape (v2.8.1) to graphically show the interactions between the 5-HT$_6$R and a network of proteins involved in the control of cytoskeletal dynamics. GPRIN1 is highlighted in pink. ERK, extracellular signal–regulated kinase; PALM, paralemmin; DOCK 3, dedicator of cytokinesis 3; WAVE1, WASP-family verprolin homologous protein 1; ARP2/3, actin-related protein 2/3; FYN, Fyn kinase. (**B**) Coimmunoprecipitation of the 5-HT$_6$R and GPRIN1 from the brain extracts of newborn 5-HT$_6$R–GFP KI mice. Western blots are representative of three independent experiments. IP, immunoprecipitation. (**C**) 5-HT$_6$R immunostaining (assessed with an anti-GFP antibody, cyan) and GPRIN1 immunostaining (magenta) in the striatum from neonatal 5-HT$_6$R–GFP KI mice. Scale bars, 5 μm. a.u., arbitrary units. Right: Line graphs generated in ImageJ using the lines represented on the merged image highlight the colocalization of both proteins at the plasma membrane in cell bodies (top), but not primary cilia (bottom). (**D** to **H**) NG108-15 cells were cotransfected with constructs encoding HA-tagged WT 5-HT$_6$R or the indicated 5-HT$_6$R mutants in the absence or presence of a GPRIN1 construct. (F and G) Cells were lysed 48 hours after transfection. (H) Cells were treated with 1 μM SB271046 (SB; which was added 24 hours after transfection and incubated for 24 hours), and the cells were lysed 48 hours after transfection. 5-HT$_6$R proteins were immunoprecipitated with agarose-conjugated anti-HA antibodies. The presence of GPRIN1 (D and F to H) or Cdk5 (E) in the immunoprecipitated samples was assessed by Western blotting analysis. Western blots are representative of three independent experiments. Bar charts show densitometric analysis of the indicated bands and are means ± SEM of three experiments. $^{**}P < 0.01$, $^{***}P < 0.001$, and $^{****}P < 0.0001$ compared to cells expressing the 5-HT$_6$R alone and exposed to vehicle. (**I**) BRET experiments measuring the interaction between the 5-HT$_6$R–YFP and Cdk5-RLuc in NG108-15 cells 24 (top) and 48 hours (bottom) after transfection. Data are from four experiments.

cAMP production 48 hours after transfection (Fig. 2A). These findings are consistent with our earlier immunoprecipitation experiments showing that the extent of the interaction between the receptor and GPRIN1 was greater 48 hours after transfection than at 24 hours after transfection. Further functional studies of the 5-HT$_6$R–GPRIN1 interaction were, thus, performed 48 hours after transfection. Consistent with a role for this interaction in the constitutive activity of the receptor, potentiation of 5-HT$_6$R–dependent cAMP production in cells coexpressing GPRIN1 was inhibited when the cells were treated with the TAT-Ct320–342 peptide (Fig. 2A). Moreover, the apparent affinity and efficacy of the inverse agonist SB271046 in inhibiting 5-HT$_6$R–dependent cAMP production were reduced in cells co-expressing GPRIN1 (Fig. 2B), suggesting that the binding of GPRIN1 may stabilize the receptor in an active conformation that exhibits a reduced affinity for inverse agonists. When cells were treated with the 5-HT$_6$R agonist WAY181187, they produced similar amounts of cAMP irrespective of the presence or absence of GPRIN1 (Fig. 2B), suggesting that constitutive, but not agonist-dependent, cAMP production depended on the physical interaction of the receptor with GPRIN1 (Fig. 2B).

To further confirm that only the constitutive and not the agonist-dependent activity of the receptor was modulated by its interaction with GPRIN1, we engineered a 5-HT$_6$R mutated at a tryptophan residue in the sixth transmembrane domain of the receptor (W281A), because

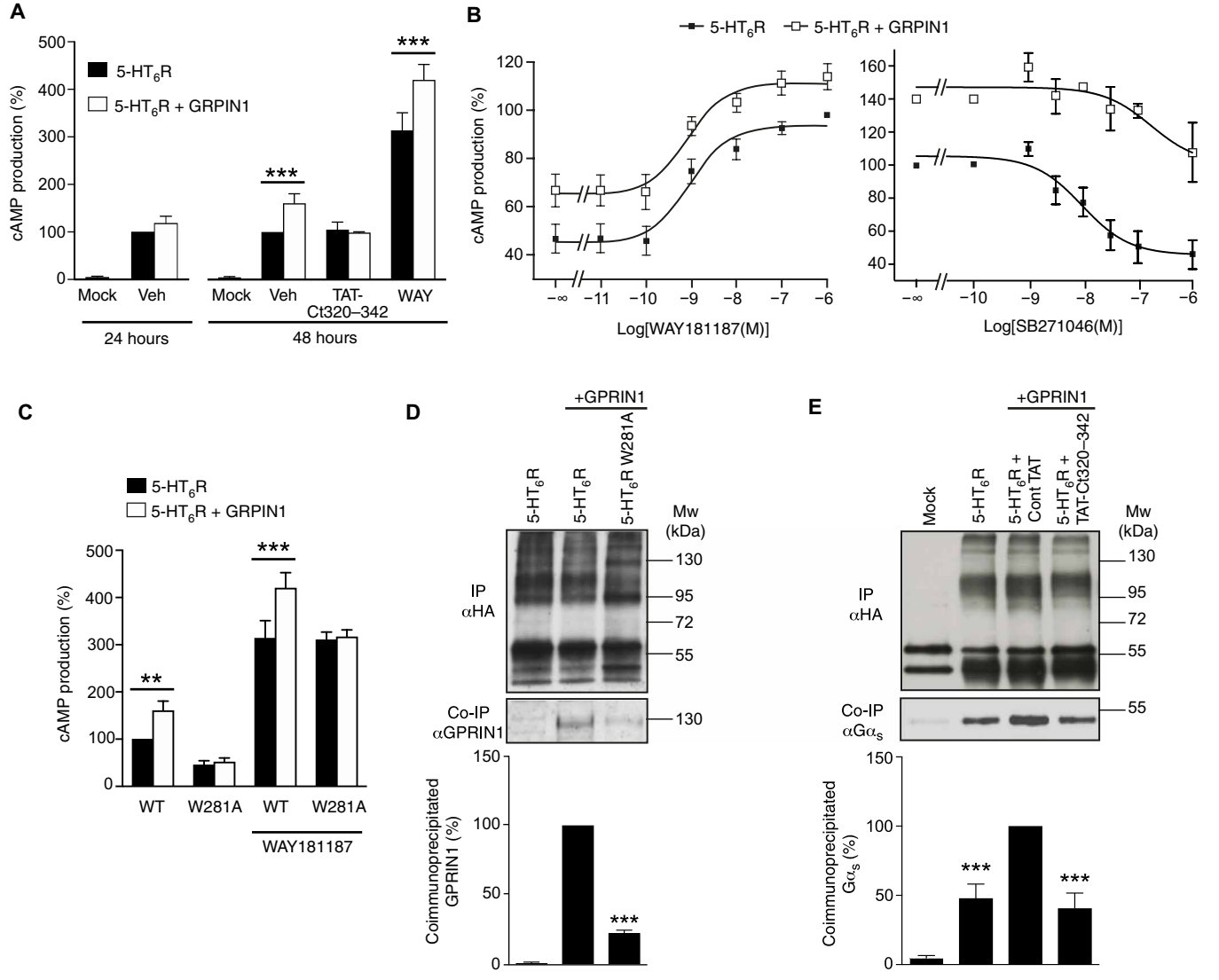

Fig. 2. GPRIN1 increases 5-HT$_6$R constitutive activity through G$_s$-cAMP signaling and promotes G$_s$ binding to the receptor in NG108-15 cells. (**A** to **C**) The CAMYEL cAMP signal was measured in NG108-15 cells transfected with constructs encoding the 5-HT$_6$R (WT or W281A mutant) alone or in combination with a GPRIN1 construct 24 (A) or 48 hours (B and C) after transfection. Cells were treated with the TAT-Ct320–342 peptide (10 μg, applied in the cell medium for 24 hours) or 1 μM WAY181187 for 5 min (A), or the indicated concentrations of either WAY181187 or SB271046 (B) or vehicle (C) for 5 min. (B) Left: Data were normalized to the amount of cAMP in cells that did not express GPRIN1 and were challenged with 1 μM WAY181187. Right: Data were normalized to the basal amount of cAMP in cells not expressing GPRIN1. Data are means ± SEM of values obtained from at least three independent experiments performed on different sets of cultured cells. $^{**}P < 0.01$ and $^{***}P < 0.001$. (**D** and **E**) NG108-15 cells were transfected with constructs encoding either HA-tagged WT or W281A 5-HT$_6$R alone or in combination with the GPRIN1 construct and lysed 48 hours after transfection. (E) Cells were treated with control TAT peptide or TAT-Ct320–342 peptide (1 μM, added 24 hours after transfection to the culture medium and incubated for 24 hours). 5-HT$_6$R proteins were immunoprecipitated with agarose-conjugated anti-HA antibodies. The presence of GPRIN1 (D) or Gα$_s$ (E) in the immunoprecipitated samples was assessed by Western blotting analysis. Western blots are representative of three independent experiments. Bar graphs show means ± SEM of immunoreactive signals measured in the three experiments. $^{***}P < 0.001$ compared to cells coexpressing WT 5-HT$_6$R and GPRIN1 (D) and compared to cells coexpressing WT 5-HT$_6$R and GPRIN1 and exposed to the control TAT peptide (E).

previous studies indicate that the corresponding tryptophan residue in 5-HT$_4$R is essential for the constitutive activity of that receptor (*42*). As expected, the constitutive activity of the W281A mutant 5-HT$_6$R was reduced compared with that of the WT receptor, whereas the agonist-dependent activity was not affected (Fig. 2C). Furthermore, GPRIN1 was unable to potentiate the residual constitutive activity of the W281A mutant 5-HT$_6$R. Immunoprecipitation experiments showed that mutation of Trp^{281} reduced the extent of the interaction between the receptor and GPRIN1 (Fig. 2D and fig. S2F), suggesting that GPRIN1 may not only enhance the constitutive activity of the 5-HT$_6$R but also preferentially associate with the receptor when it is in its active conformational state.

The increase in the constitutive activity of the receptor could result either from the increased recruitment of activated G protein by the receptor in the presence of GPRIN1 or from an increase in abundance of the receptor at the plasma membrane. To discriminate between these two possibilities, we compared the membrane abundance of the receptor in NG108-15 cells in the presence or absence of GPRIN1.

We found no substantial difference in the membrane abundance of the receptor in either cell population (fig. S4). Furthermore, the amount of G_s protein that coimmunoprecipitated with the receptor was increased in the presence of GPRIN1, an effect that was prevented by treatment of the cells with the TAT-Ct320–342 peptide (Fig. 2E and fig. S2G). These results suggest that the GPRIN1-dependent increase in 5-HT_6R constitutive activity results from enhanced G_s signaling by the receptor rather than an increase in its abundance at the plasma membrane.

GPRIN1 enhances 5-HT_6R–dependent neurite elongation and branching in NG108-15 cells

We previously demonstrated that the 5-HT_6R induces the initiation of neurite growth in NG108-15 cells in a ligand- and cAMP-independent manner, through a Cdk5-Cdc42 pathway (*20*). Consistent with previous studies showing that GPRIN1 can also induce neurite growth (*31*–*33*), we sought to determine whether GPRIN1 promoted neurite growth in NG108-15 cells expressing the 5-HT_6R. Immunocytochemistry experiments with NG108-15 cells transfected with cDNAs encoding either GFP or the GFP-fused receptor, alone or in combination with GPRIN1, showed that 24 hours after transfection, coexpression of GPRIN1 did not further increase the length of neurites when compared with the length of neurites produced by cells expressing the receptor alone (Fig. 3A). Consistent with our previous findings, 5-HT_6R–dependent neurite growth was reduced when a dominant-negative mutant Cdk5 was coexpressed (Fig. 3A), suggesting that the initiation of neurite growth did not depend on the presence of GPRIN1 but required the kinase activity of Cdk5. In contrast, 48 hours after transfection, cells expressing both 5-HT_6R and GPRIN1 exhibited longer and more branched neurites than did cells expressing the receptor alone, as determined by immunocytochemistry and quantified by Sholl analysis (Fig. 3A). Furthermore, coexpression of the dominant-negative mutant Cdk5 did not affect the GPRIN1-induced increase in branching at that stage of neuronal differentiation, although a residual effect on neurite length was seen (Fig. 3B). This suggests that the branching of neurites does not require the activity of Cdk5 and is consistent with our results showing that Cdk5 does not interact with the receptor 48 hours after transfection.

Treating cells coexpressing 5-HT_6R and GPRIN1 with the TAT-Ct320–342 peptide or coexpressing the 5-HT_6R S350D mutant with GPRIN1 abolished the effect of GPRIN1 on both neurite extension and branching (Fig. 3, A and B, and fig. S3C), indicating that the growth-promoting effects of GPRIN1 depended on its physical interaction with the 5-HT_6R. Last, the constitutive activity of the receptor was also required, as shown by the lack of effect of GPRIN1 in cells cotransfected with the W281A mutant 5-HT_6R, which exhibits reduced constitutive activity compared with that of the WT receptor (Fig. 3, A and B). This latter result prompted us to explore whether the length of neurites in NG108-15 cells correlated with the abundance of cAMP; thus, we plotted the neurite length of cells as a function of the extent of 5-HT_6R constitutive activity. As expected, there was no correlation between these two factors in cells 24 hours after transfection, whereas 48 hours after transfection, neurite length positively correlated with the extent of constitutive activity of the 5-HT_6R (Fig. 3C). Further supporting the link between neurite growth, branching, and cAMP production resulting from the constitutive activity of the 5-HT_6R, neurite length and branching in NG108-15 cells coexpressing GPRIN1 with the mutant 5-HT_6R incapable of activating G proteins were reduced compared with those in cells coexpressing GPRIN1 with the WT receptor (Fig. 3, D and E). Moreover, treating cells coexpressing the WT receptor with the 5-HT_6R antagonist SB271046, the membrane-permeable cAMP analog RPcAMP, or KT 5720 [both of which are inhibitors of cAMP-dependent protein kinase (PKA)] also prevented GPRIN1-dependent neurite growth and branching (Fig. 3, D and E), whereas none of these treatments affected neurite architecture in cells expressing the receptor alone. This finding suggests that neurite elongation and branching depend on the activation of PKA stimulated by agonist-independent, 5-HT_6R–dependent cAMP production, which itself requires the physical interaction of GPRIN1 with the receptor. Consistent with our previous study (*20*), there was no effect of the G protein coupling–defective triple receptor mutant or of treatment with RPcAMP on neurite length 24 hours after transfection (fig. S5).

The GPRIN1–5-HT_6R interaction promotes neurite elongation and branching in neurons

We next sought to determine whether the interaction between the native 5-HT_6R and GPRIN1 likewise promoted neurite elongation and branching in primary cultured neurons. We performed these experiments on striatal neurons, which express large amounts of 5-HT_6R density and GPRIN1 (Fig. 4). We first infected striatal neurons with lentiviruses encoding two different short hairpin RNAs (shRNAs) directed against GPRIN1. Both shRNAs led to a nearly total loss of GPRIN1 protein detection by Western blotting (Fig. 4A). Furthermore, knocking down GPRIN1 statistically significantly decreased both neurite length and the complexity of mature striatal neurons (Fig. 4B), as assessed by Sholl analysis on neurons grown for 13 days in vitro (DIV), reminiscent of what was observed in transfected NG108-15 cells. We next exposed striatal neurons to the TAT-Ct320–342 peptide to disrupt the interaction between GPRIN1 and 5-HT_6R. This treatment resulted in a marked decrease in neurite length and complexity as compared with neurons treated with a control TAT peptide (Fig. 4C), suggesting that the interaction between endogenous GPRIN1 and 5HT_6R is necessary to promote neurite growth and branching in striatal neurons. We then compared, from DIV 1 to DIV 4, the neurite length of neurons treated with either the TAT-Ct320–342 peptide or the control TAT peptide. We found a statistically significant reduction in neurite length as early as DIV 2 in neurons exposed to the TAT-Ct320–342 peptide, and this reduction was further enhanced at DIVs 3 and 4 (fig. S6A). Last, reminiscent of the observations made in NG108-15 cells, neurons treated with RPcAMP also showed a marked decrease in neurite length measured at DIV 4 (fig. S6B).

DISCUSSION

Studies have demonstrated that the 5-HT_6R plays crucial roles in both the correct migration and positioning of neurons, as well as in the initiation of neurite growth (*19*, *20*, *43*). These effects, which are mostly independent of the canonical G_s-cAMP pathway, prompted the use of unbiased interactomics studies to identify previously uncharacterized signaling proteins recruited by the receptor and alternative signaling pathways underlying its control of neurodevelopmental processes. These studies revealed that Cdk5 binds to the C-terminal domain of the receptor to promote neurite growth initiation through an agonist-independent mechanism involving the phosphorylation of Ser^{350} in the receptor, which in turn leads to activation of the small GTPase (guanosine triphosphatase) Cdc42 (Fig. 5) (*20*). Here, we

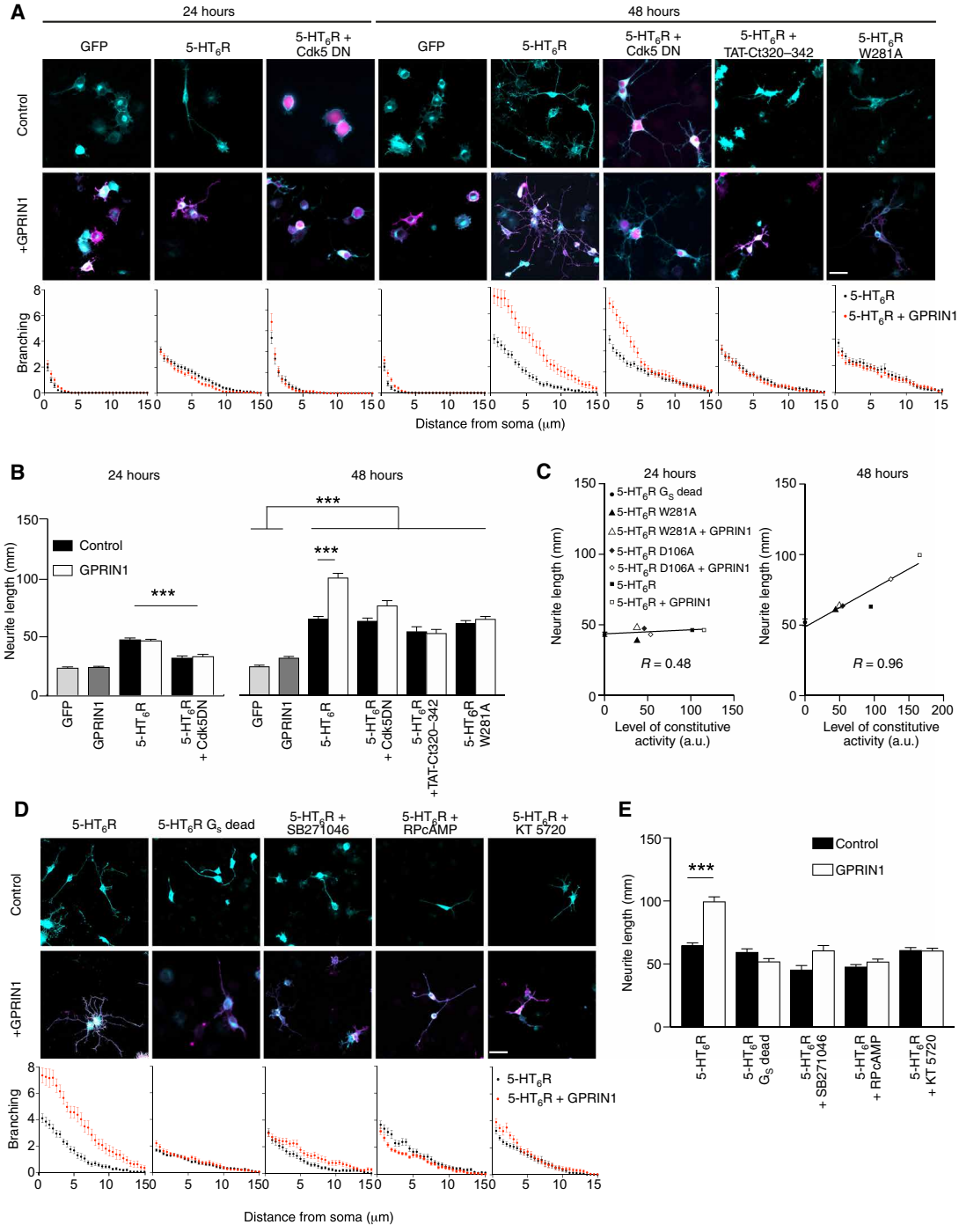

Fig. 3. GPRIN1 interaction with the 5-HT$_6$R promotes neurite growth and branching in a PKA-dependent manner in NG108-15 cells. (**A**) NG108-15 cells were transfected with plasmids encoding GFP or YFP-tagged WT or W281A 5-HT$_6$R alone or in combination with constructs encoding a dominant-negative Cdk5 mutant (Cdk5-DN; top) or GPRIN1 (bottom). GFP or receptor labeling is shown in cyan; GPRIN labeling is shown in magenta. Where indicated, cells were treated for 24 hours with the TAT-Ct320–342 peptide (1 μM). The images show fields representative of three independent experiments performed on different cultures. Scale bar, 50 μm. The graphs represent the branching index, measured as the number of intersections between dendrites and an overlaid concentric sphere, as a function of the distance from the soma. (**B**) Histogram showing the quantification of neurite length (μm) in NG108-15 cells expressing the corresponding constructs and that were left untreated or were incubated with the TAT-Ct320–342 peptide. At least 300 neurites were analyzed per condition. ***$P < 0.001$. (**C**) Correlation plots between neurite length and basal cAMP amounts in NG108-15 measured either 24 (left) or 48 hours (right) after transfection of the cells with the indicated constructs. (**D**) NG108-15 cells were transfected with plasmids encoding YFP-tagged WT 5-HT$_6$R or a mutant receptor incapable of coupling to G protein (G_s dead) alone or in combination with the GPRIN1 construct. Cells expressing the WT receptor were treated for 24 hours with 1 μM SB271046, 25 μM RPcAMP, or 2 μM KT 5720. Cells were lysed 48 hours after transfection. Representative fields of three independent experiments performed on different sets of cultured cells are shown. Scale bar, 50 μm. The graphs represent the branching index, which was measured as described in (A). (**E**) The histogram shows the quantification of neurite length in the indicated conditions, which were from the experiments shown in (D). ***$P < 0.001$.

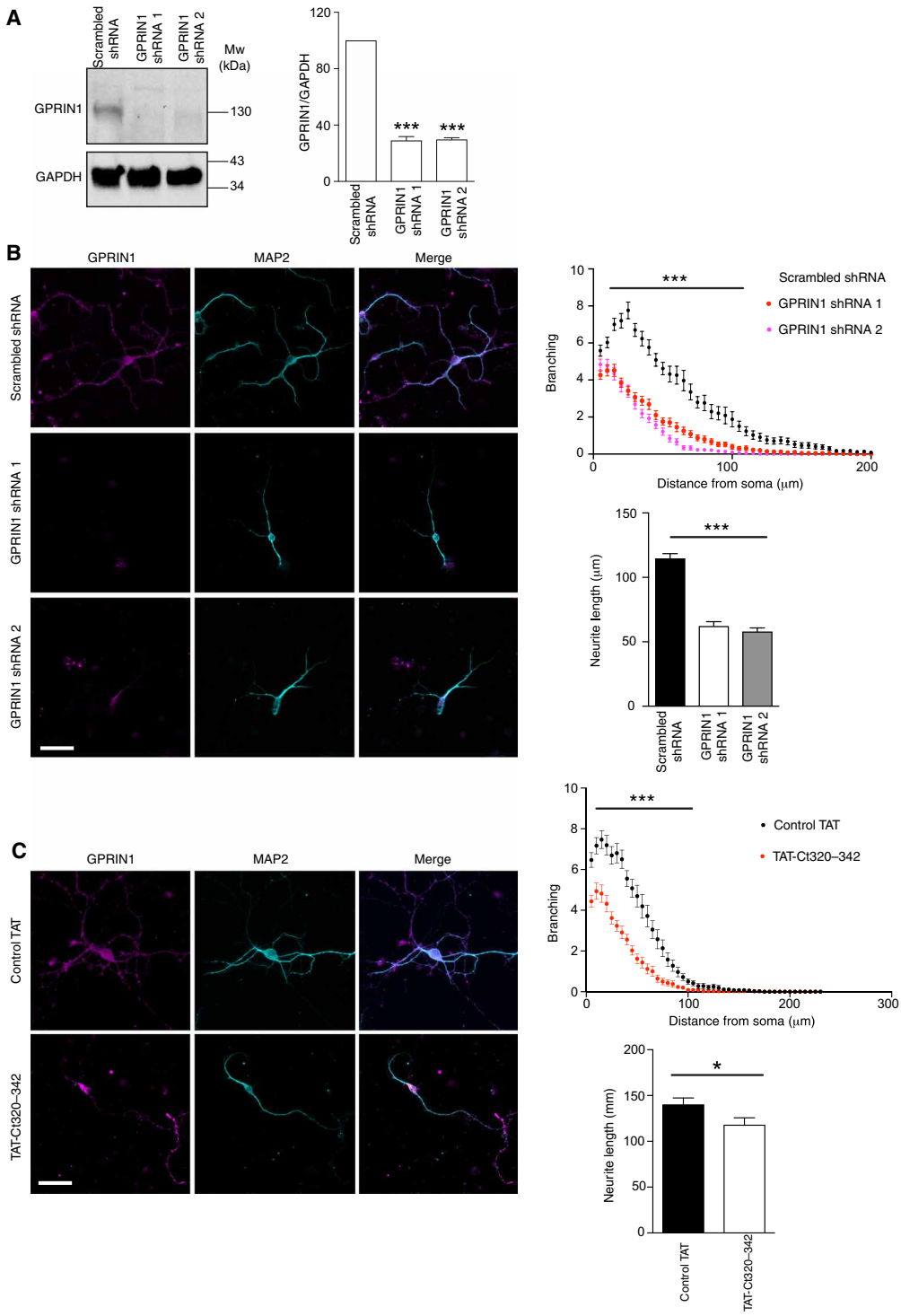

Fig. 4. Interaction between endogenous 5-HT$_6$R and GPRIN1 promotes neurite extension and the branching of striatal neurons. (**A**) Knockdown of GPRIN1 after infection of cultured mouse striatal neurons at DIV 4 by a virus expressing either control or two different GPRIN1-specific shRNAs. The neurons were lysed at DIV 13, and GPRIN1 was detected by Western blotting analysis. The bar graph shows the mean ± SEM of the GPRIN1 immunoreactive signal [normalized to the glyceraldehyde-3-phosphate dehydrogenase (GAPDH) immunoreactive signal] in each condition. ***$P < 0.001$ compared to neurons expressing the scrambled shRNA. (**B**) Neurons were infected with either control (top) or GPRIN1-specific (middle and bottom) shRNAs. Neurons were fixed at DIV 13. GPRIN1 immunoreactivity is shown in magenta, and MAP2 immunoreactivity in cyan. Scale bar, 5 μm. The graph shows the measurement of neurite branching, as assessed by the Sholl analysis. The bar graph shows neurite length for neurons infected with control (black bar) or GPRIN1-specific shRNAs (white and gray bars). For both branching and neurite length, data are means ± SEM of three independent experiments performed from different sets of cultured neurons with at least 300 neurites measured per conditions. ***$P < 0.001$. (**C**) Neurons were treated with either the control TAT peptide (top) or the TAT-Ct320–342 peptide (1 μM, added to cultures at DIV 4; bottom), and fixed at DIV 13. GPRIN1 is shown in magenta, and MAP2 in cyan. Neurite branching and length were determined and plotted as described in (B). *$P < 0.05$.

showed that the 5-HT$_6$R C-terminal domain also recruited GPRIN1, a Cdk5 substrate initially identified in a cDNA bank screen designed to find previously uncharacterized partners of Gα subunits (*30*, *44*). Two other variants (GPRIN2 and GPRIN3) have been described, but only GPRIN1 was identified in the 5-HT$_6$R interactome. GPRIN1 is mainly found in the central nervous system, where it is expressed by neurons but not glial cells. Its expression is high during embryonic development, with a peak at E16.5. It is still found in the adult brain, but only in the hippocampus, ventral striatum, and some cortical regions (*34*), which greatly overlaps with the expression pattern of the 5-HT$_6$R. Corroborating these observations, we found that the receptor forms a complex with GPRIN1 in mouse brain at the neonatal stage, a critical period for neuronal differentiation and wiring of neuronal networks (*45*). At that stage of neural development, receptors are found not only in the primary cilium, as previously described (*36*, *39*, *46*), but also in the soma of neurons, where they are mainly detected at the plasma membrane. However, we did not detect GPRIN1 in primary cilia, suggesting that only the receptor pool found outside the cilium is engaged in complexes with GPRIN1.

The GPRIN1 association with the 5-HT$_6$R, which occurred in the absence of agonist, was reduced in cells treated with the 5-HT$_6$R antagonist SB271046, which acted as an inverse agonist toward receptor-stimulated G$_s$-cAMP signaling (Fig. 2A). These results suggest that the 5-HT$_6$R–GPRIN1 interaction is dynamically

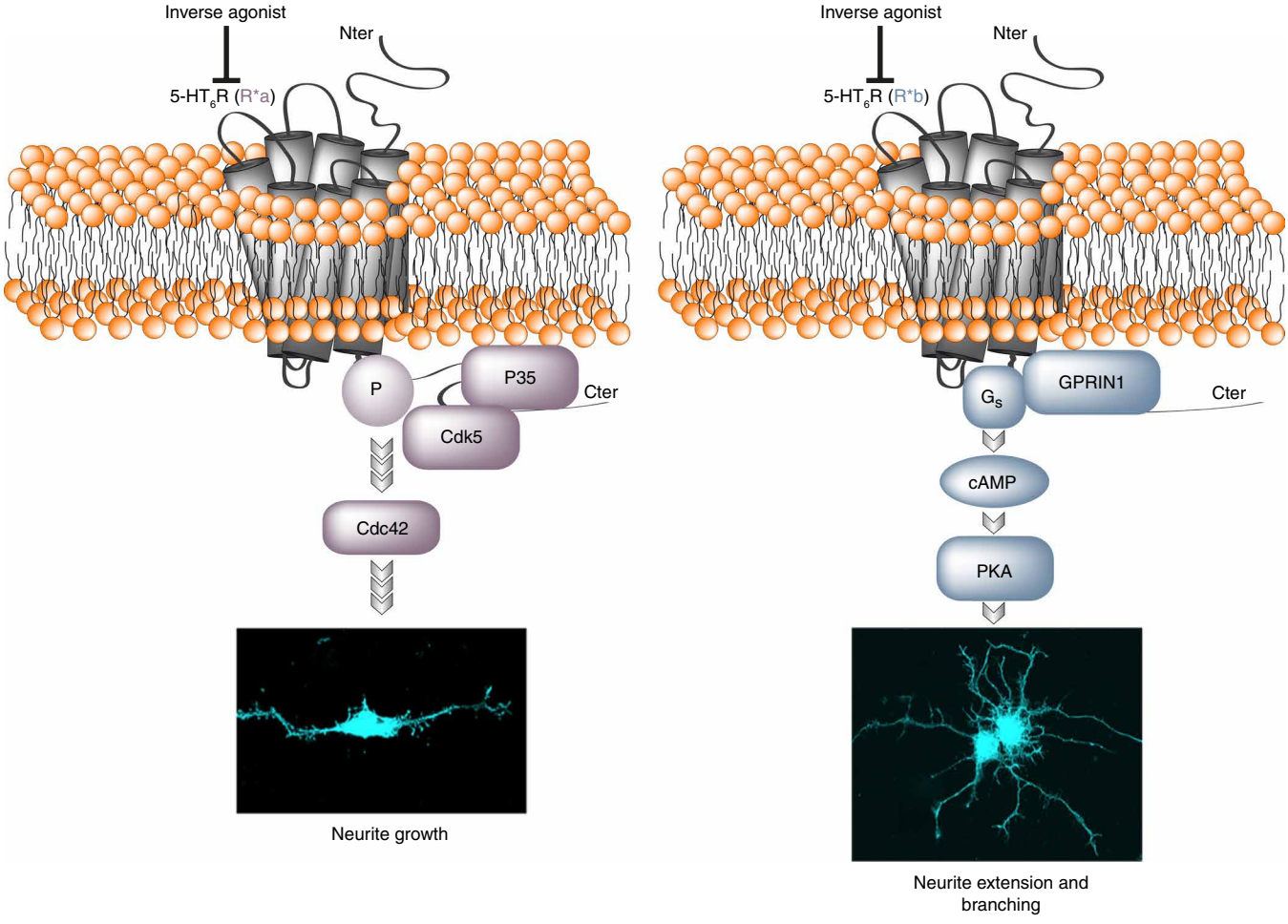

Fig. 5. Schematic representation of the sequential interaction between the 5-HT$_6$R and either Cdk5 or GPRIN1 and its consequence on agonist-independent 5-HT$_6$R–stimulated signaling. Association of the 5-HT$_6$R with Cdk5 results in receptor phosphorylation on a serine residue located in the receptor C-terminal (Cter) domain, a necessary step in the agonist-independent, receptor-mediated activation of Cdc42 signaling and initiation of neurite outgrowth (left), whereas the association of the receptor with GPRIN1 promotes the recruitment of activated Gα_s and neurite extension and branching through an agonist-independent, PKA-dependent mechanism (right). Nter, N-terminal. The application of an inverse agonist inhibits both pathways, indicating that these are dependent on the receptor's constitutive activity.

regulated by the conformational state of the receptor and that a specific receptor conformation in the absence of ligand is favorable for GPRIN1 recruitment. Consistent with this hypothesis, mutating a tryptophan residue essential for 5-HT$_6$R constitutive activity to an alanine reduced the interaction between the receptor and GPRIN1.

GPRIN1 not only associated with the 5-HT$_6$R in its active conformation but also enhanced the constitutive activity of the receptor leading to G$_s$ signaling (Figs. 1G and 2, A and B). Furthermore, we showed that GPRIN1 promoted the recruitment of Gα_s protein by 5-HT$_6$R (Fig. 2E). Previous studies showed that GPRIN1 preferentially interacts with activated Gα proteins of the G$_{i/o}$ subfamily (*35*). Assuming that GPRIN1 likewise associates with activated Gα_s, we hypothesize that GPRIN1 favors the recruitment of Gα_s by active receptor conformations, resulting in the formation of a ternary complex comprising 5-HT$_6$R, GPRIN1, and active Gα_s, thus promoting receptor constitutive activity. Alternatively, the association of GPRIN1 with the 5-HT$_6$R might induce a conformational change in the receptor toward a more active state exhibiting a higher level of constitutive activity through G$_s$ signaling.

Together, our current and previous findings (*20*) demonstrate a high level of 5-HT$_6$R constitutive activity toward both canonical G$_s$ signaling and G protein–independent signaling, which depends on allosteric modulations by interacting proteins. To our knowledge, these data provide one of the few examples of the modulation of the constitutive activity of a GPCR by GIPs. Other examples are the constitutive activity of type I metabotropic glutamate receptors (mGluRs), which can be modulated by Homer proteins, and the constitutive activity of the ghrelin receptor growth hormone secretagogue receptor 1a (GHSR1a), which can be regulated by the melanocortin receptor accessory protein subunit 2 (MRAP2) (*47*, *48*). However, in contrast to our current findings, the association of Homer3 with the C-terminal domain of mGluR1 or mGluR5 prevents rather than promotes the constitutive activity of either receptor, whereas the expression of the short, inducible form of Homer (Homer1a) results, indirectly through the disruption of mGluR1- or mGluR5-Homer3 complexes, in the enhanced constitutive activity of mGluR1 or mGluR5. In the case of GHSR1a, the interaction with MRAP2 results in biased signaling, enhancing receptor signaling through G$_q$, while blocking both its constitutive activity and the recruitment of

β-arrestin. Our data also suggest that constitutive 5-HT_6R activation can result from different mechanisms depending on the nature of the associated GIP: Agonist-independent engagement of Cdk5-Cdc42 signaling depends on receptor phosphorylation at Ser^{350} by receptor-associated Cdk5, whereas the activation of G_s signaling by GPRIN1 might result from an enhanced recruitment of activated $G\alpha_s$ or a switch to a more active conformational state of the receptor.

The interactions of 5-HT_6R with Cdk5 and GPRIN1 seem to occur sequentially to facilitate a fine temporal regulation of key neurodevelopmental processes (Fig. 5). Previous studies showed that the agonist-independent activation of Cdk5 by 5-HT_6R early during brain development is essential for the normal positioning of cortical neurons, indicating a fine control of the migration process (*19*, *43*). Beyond migration, the association of 5-HT_6R with Cdk5 also promoted the initiation of neurite growth (*20*), which is consistent with previous studies performed in pheochromocytoma (PC12) cells, for which the initiation of neurite growth is cAMP independent (*49*). At a later stage of neuronal differentiation, the 5-HT_6R might associate with GPRIN1 to induce neurite elongation and branching. This sequential association of 5-HT_6R with Cdk5 and GPRIN1, initially established in transfected NG108-15 cells, likely occurs between native proteins in primary neurons. Inhibiting agonist-independent activation of Cdk5/Cdc42 signaling induced by the 5-HT_6R prevented the initiation of neurite growth measured during the first 24 hours after neuron seeding, whereas knockdown of GPRIN1 or disruption of the 5-HT_6R–GPRIN1 interaction at later stage of neuronal differentiation (between 2 and 13 days after plating) prevented further neurite elongation and branching. These findings provide an example of functionally relevant dynamic interactions between a GPCR and several GIPs. The cellular mechanisms underlying the sequential interaction of 5-HT_6R with Cdk5 and GPRIN1 remain to be elucidated. As previously mentioned, Cdk5-mediated initiation of neurite growth depends on the phosphorylation of the 5-HT_6R on Ser^{350} by associated Cdk5. We also identified in the 5-HT_6R interactome the protein phosphatase PP2A, which dephosphorylates Cdk5 targets (*50*). Because PKA can phosphorylate and activate PP2A (*51*), we hypothesize that constitutively active 5-HT_6R might promote the activation of PP2A through PKA, leading to the dephosphorylation of Ser^{350} and the release of Cdk5, thus facilitating interaction with GPRIN1. The 5-HT_6R might also interact with either Cdk5 or GPRIN1 depending on their respective subcellular localization. Because both 5-HT_6R and Cdk5 activation increase cilial length, one can speculate that the formation of 5-HT_6R–Cdk5 complexes occurs in the primary cilium or cellular compartments involved in primary cilium morphogenesis (for example, the distal centriole appendages), whereas GPRIN1 associates with receptors located in the soma of neurons.

A viable GPRIN1 knockout (KO) mouse model has been described. Cultured neurons from GPRIN1 KO mice show reduced firing activity compared with neurons from WT mice, and adult GPRIN1 KO mice display altered learning performance (*52*), a phenotype possibly reflecting defects in neurite growth and early neuronal network shaping. Although initial studies showed the ability of GPRIN1 bound to activated $G\alpha_{i/o}$ proteins to promote neurite growth through the activation of Cdc42 (*33*, *35*), our data together with previously published results suggest that its neurite growth–promoting effects tightly depend on its interaction with membrane receptors (*31*–*33*). Only the coexpression of GPRIN1 and 5-HT_6R induced a substantial effect upon neurite elongation and branching in NG108-15 cells, whereas expression of GPRIN1 alone only induced a marginal effect upon neurite growth. Similarly, the association of GPRIN1 with the μ-opioid receptor (MOR) potentiates receptor-mediated neurite growth by targeting MOR tethered with activated $G\alpha_i$ to lipid rafts (*31*), whereas the interaction of GPRIN1 with the α7 nicotinic receptor targets the receptor to growth cones and increases its plasma membrane localization, which results in longer and more complex neurites (*31*). The signaling mechanisms underlying neurite growth under the control of GPRIN1 might also depend on the nature of the receptor with which GPRIN1 is associated. Whereas neurite growth under the control of the α7-GPRIN1 complex seems to involve a Ca^{2+}/CaM-kinase II/phosphatase 2B pathway (*32*), the 5-HT_6R–GPRIN1 complex promotes neurite elongation and branching through a cAMP- and PKA-dependent mechanism.

In conclusion, our study provides an example of dynamic associations between a GPCR and several of its GIPs to ensure highly coordinated cellular processes such as the growth initiation, extension, and branching of neurites. These findings further highlight the allosteric properties of GPCRs, which can adopt many active and physiologically relevant conformations, some of them being stabilized upon interaction with GIPs in the absence of orthosteric agonists.

MATERIALS AND METHODS

Animals

5-$HT_6^{GFP/GFP}$ KI mice (*29*) were generated at the Institut Clinique de la Souris (Illkirch-Graffenstaden, France) and were used for GFP-TRAP and immunohistochemistry experiments. Primary cultures of neurons were realized from OF1 (Oncins-France 1) mouse embryos originating from Charles River. Procedures were performed in strict compliance with the animal use and care guidelines of Montpellier University (authorization D34-172-4).

Plasmids, chemicals, and antibodies

The human hemagglutinin (HA)–tagged WT 5-HT_6R construct was previously described (*25*, *53*). The human YFP-tagged 5-HT_6R construct was provided by S. Morisset (Centre de Biophysique Moléculaire, Orléans, France). 5-HT_6R mutants were generated by site-directed mutagenesis and assessed by sequencing. Plasmid encoding human GPRIN1 was purchased from Sigma-Aldrich, and the peGFPC1 plasmid was from Clontech. The viral constructs encoding two different shRNAs directed against GPRIN1, subcloned into the pLKO vector, were obtained from Sigma-Aldrich, and pLKO enhanced GFP (eGFP) was obtained from the virus production platform of Montpellier (PVM, BioCampus, Montpellier, France). Viral particles were produced by the PVM platform. The agarose-conjugated anti-HA antibody (clone no. HA-7) was purchased from Sigma-Aldrich, GFP-TRAP beads were from Chromotek, the rabbit anti-GPRIN1 antibody was from Proteintech (ref 13771-1-AP), the rabbit anti-$G\alpha_s$ antibody was from Calbiochem (ref 371732), the rat anti-HA antibody (clone 3F10) was from Roche, the mouse anti-MAP2 (microtubule-associated protein 2) antibody (clone [HM2], ref ab11267) was from Abcam, and the mouse anti-Arl13b (clone N295B/66, ref 75-287) was from Antibodies Incorporated. For GFP labeling, we used the chicken polyclonal anti-GFP antibody (A10262, ref 10524234) from Thermo Fisher Scientific or the rabbit polyclonal anti-GFP antibody (ref PABG1) from Chromotek. WAY181187, SB271046 hydrochloride, KT 5720, and cAMPS-Rp triethylammonium salt were purchased from Tocris Biosciences. Coelenterazine h (used for

BRET experiments) was purchased from Nanolight Technology (ref 50909-86-9). The CAMYEL probe and the derivatized benzyl guanine labeled with europium cryptate (BG-K) or d2 (BG-d2) as acceptor were provided by the pharmacological screening facility (ARPEGE, BioCampus, Montpellier, France). Interfering peptides (>90% purity) were purchased from GenScript. Peptide sequences were as follows: TAT-Ct320–342 peptide: YGRKKRRQRRRPLFMRDFKRALGRFLPCPRCPR; TAT control peptide: GRKKRRQRRRPCRPCPLFRGLARKFDRMFLP.

Cell culture, transfection, and treatments

NG108-15 cells were grown in Dulbecco's modified Eagle's medium (DMEM) supplemented with 10% dialyzed fetal bovine serum (FBS), 2% hypoxanthine/aminopterin/thymidine (Life Technologies), and antibiotics. Cells were transfected in suspension using Lipofectamine 2000 (Life Technologies) with plasmids encoding GFP, WT, or mutant HA–5-HT_6Rs with or without the plasmid encoding GPRIN1. After transfection, cells were maintained in DMEM supplemented with 2% dialyzed FBS and treated as indicated in the figure legends either 5 or 24 hours after transfection. The cells were used either 24 or 48 hours after transfection for all experiments. Primary cultures of striatal neurons were prepared from E15.5 OF1 mouse embryos. Striata were dissociated by manual trituration, and cells were plated onto polyornithine- and laminin-coated 12-mm glass coverslips in 24-well plates. Cultures were maintained in Neurobasal medium (Thermo Fisher Scientific) supplemented with 10 ml of B27 supplement (Gibco, ref 17504-044), 0.2 mM GlutaMAX, with 0.2 mM glutamine and penicillin (100 U)/streptomycin (100 μg) and kept at 37°C in a humidified atmosphere containing 5% CO_2. For branching experiments, neurons were transfected at DIV 1 with cDNA encoding GFP to visualize dendritic trees, treated at DIV 4 as indicated in the figure legends, and fixed at DIV 13.

Immunocytochemistry and morphological analyses

NG108-15 cells or neurons, grown on coated glass coverslips, were fixed in paraformaldehyde (PFA; 4% for 10 min for NG108-15 cells and 2% for 15 min for neurons). Cells were then successively incubated with primary antibodies (mouse anti-MAP2, 1:1000; rabbit anti-GPRIN1, 1:500; or rat anti-HA, 1:1000) and with secondary antibodies (Alexa Fluor 488–conjugated anti-mouse or Alexa Fluor 594–conjugated anti-rabbit, 1:1000). For labeling of the 5-HT_6R in cultured neurons, tyramide amplification of the signal given by the rabbit polyclonal antibody (1:1000) was performed using the Invitrogen Alexa Fluor 488 Tyramide SuperBoost Kit (ref 15631902) according to the manufacturer's protocol. Coverslips were mounted in Mowiol. Images were captured with an Axio Imager Z1 microscope equipped with epifluorescence (Zeiss), using a 20× objective. Neurites were detected on the basis of MAP2 staining or GFP expression. Neurite length was measured using the NeuronJ plugin of ImageJ software. A minimum of 15 fields of cells originating from three independent cultures were analyzed per condition. Branching was assessed using a semiautomated Sholl analysis with 5-μm ring intervals starting at 5 μm from the soma (SynD, MATLAB). A minimum of 45 cells originating from three independent cultures were analyzed for each condition.

Immunohistochemistry on brain slices

Mice were rapidly anesthetized with isoflurane and perfused transcardially with 0.1 M phosphate-buffered sodium (PBS; pH 7.5). Brains were then fixed in 4% PFA diluted in PBS for 24 hours at 4°C and then incubated successively in 10, 20, and 30% (w/v) sucrose diluted in PBS for cryoprotection. Sixteen-micrometer-thick sections were cut with a cryostat (Leica), deposited directly on slides, and stored at −80°C until use. For immunolabeling experiments, sections were thawed at room temperature and rehydrated for 15 min in PBS. Sections were blocked for 2 hours in PBS containing 0.2% (v/v) Triton X-100, 3% (w/v) bovine serum albumin (BSA; A2153, Sigma-Aldrich), and then incubated overnight at room temperature in primary antibody solution containing 1:1000 anti-GFP from chicken (A10262, Invitrogen) and 1:500 anti-GPRIN1 from rabbit (13771-1-AP, Proteintech) in PBS, 0.2% Triton X-100, 1% BSA. Sections were then washed three times for 30 min each in PBS and incubated with Alexa Fluor 488–coupled goat anti-chicken and Cy3-coupled goat anti-rabbit secondary antibodies (1:1000) for 2 hours at room temperature. Sections were washed three times for 30 min each in PBS, dried, and mounted in DPX mountant (Sigma-Aldrich, ref 06522). Images were acquired with a Leica SP8 confocal microscope equipped with an oil-immersed 63× objective, with a 2048 × 2048 resolution (excitation lasers, 488 and 561 nm; acquisition filters, 500 to 539 and 572 to 617 nm, respectively).

Immunoprecipitation experiments

Whole brains from newborn mice were washed in PBS and homogenized by potterization. The samples were centrifuged at 3000*g* for 10 min at 4°C. Pellets were resuspended in solubilization buffer containing 10 mM tris-HCl (pH 7.4), 150 mM NaCl, 0.5 mM EDTA, 0.4% dodecyl maltoside, 0.5% Triton X-100, and a protease cocktail inhibitor (Roche). Samples were left to solubilize at 4°C for 4 hours and then were centrifuged for 30 min at 13,000*g* at 4°C. Protein concentration was measured using a bicinchoninic assay (BCA, Sigma-Aldrich), and solubilized proteins were used for GFP-TRAP assays (Chromotek). Transfected NG108-15 cells were lysed in a solubilization buffer containing 20 mM Hepes (pH 7.4), 150 mM NaCl, 1% NP-40, 10% glycerol, dodecyl maltoside (4 mg/ml), phosphatase inhibitors (10 mM NaF, 2 mM sodium orthovanadate, 1 mM sodium pyrophosphate, and 50 mM β-glycerophosphate), and a protease inhibitor cocktail (Roche) for 1 hour at 4°C. Samples were centrifuged at 15,000*g* for 15 min at 4°C, and supernatants containing solubilized proteins were used for immunoprecipitation. Solubilized proteins (1 mg per condition) were incubated either with agarose-conjugated anti-HA antibody or GFP-TRAP beads overnight at 4°C. The beads were washed five times with lysis buffer for anti-HA beads or with a washing buffer specified by the manufacturer protocol for GFP-TRAP beads [10 mM tris/Cl (pH 7.5), 150 mM NaCl, and 0.5 mM EDTA]. Immunoprecipitated proteins were then eluted in Laemmli sample buffer and analyzed by Western blotting.

Western blotting analysis

Proteins were separated on 10% polyacrylamide gels and then were transferred to Hybond C nitrocellulose membranes (GE Healthcare). Membranes were first incubated with the appropriate primary antibodies (rabbit anti-GPRIN1, 1:500; rabbit anti-$G\alpha_s$, 1:500; rat anti-HA, 1:1000) and then with horseradish peroxidase (HRP)–conjugated anti-rat or anti-rabbit secondary antibodies (1:5000; GE Healthcare). Immunoreactivity was detected with an enhanced chemiluminescence method (ECL plus detection reagent, GE Healthcare) and imaged with a ChemiDoc system (Bio-Rad). Immunoreactive bands were quantified by densitometry using Image Lab software (Bio-Rad).

BRET experiments

NG108-15 cells were transfected in white 96-well microplates (Greiner) with a fixed amount of Cdk5-RLuc (Renilla-luciferin 2-monooxygenase) plasmid and an increasing concentration of 5-HT$_6$R–YFP construct (from 0 to 20 ng per well). The BRET signal from each plate was first analyzed 24 hours after the transfection and then again at 48 hours. We collected BRET measurements 2 min after the addition of the luciferase substrate coelenterazine h at a final concentration of 5 μM. Luminescence and fluorescence were detected with the Mithras LB 940 Multireader (Berthold), which enables the sequential integration of luminescence signals detected with two filter settings (RLuc filter, 485 ± 10 nm; YFP filter, 530 ± 12 nm). Emission signals at 530 nm were divided by emission signals at 485 nm. The BRET ratio was defined as the difference between the emission ratio obtained with cotransfected RLuc and YFP fusion proteins and that obtained with the RLuc fusion protein alone. The results were expressed in milliBRET units (mBU; with 1 mBU corresponding to the BRET ratio values multiplied by 1000). Total fluorescence and luminescence were used as relative measures of total amounts of the YFP- and RLuc-tagged proteins, respectively. BRET signals were plotted as a function of the ratio between total fluorescence and total luminescence ratio.

cAMP measurements

cAMP measurement was performed in NG108-15 cells transiently expressing 5-HT$_6$R using the BRET sensor for cAMP, CAMYEL (cAMP sensor using YFP-Epac-RLuc) (*41*). NG108-15 cells were cotransfected in suspension with the 5-HT$_6$R and CAMYEL constructs using Lipofectamine 2000 according to the manufacturer's protocol and plated in white 96-well plates (Greiner) at a density of 80,000 cells per well. Twenty-four hours after transfection, the cells were washed with PBS containing calcium chloride and magnesium chloride (Gibco, ref 14040-091). Coelenterazine h was added at a final concentration of 5 μM. Plates were incubated at room temperature for 5 min before BRET measurements. BRET was measured using a Mithras LB 940 plate reader. Expression of 5-HT$_6$R in NG108-15 cells induced a decrease in the CAMYEL BRET signal compared to that in cells transfected with an empty vector. This decrease in CAMYEL BRET signal was used as an index of 5-HT$_6$R constitutive activity through G_s signaling.

Measurement of cell surface 5-HT$_6$R by time-resolved–fluorescence resonance energy transfer

These experiments were performed as described previously (*54*). NG108-15 cells were transfected with plasmid encoding a soluble NSF attachment protein (SNAP)–tagged 5-HT$_6$R with or without plasmid encoding GPRIN1 or were transfected with an empty plasmid. Forty-eight hours after transfection, the cells were plated in a Greiner CELLSTAR 96-well plate (at 50,000 cells per well) and washed with PBS supplemented with calcium chloride and magnesium chloride (Gibco, ref 14040-091). The cells were then labeled with derivatized benzyl guanine (BG-K or BG-d2) for 1 hour at 37°C in a humidified atmosphere containing 5% CO_2. After labeling, the cells were washed four times with PBS. The emission signal from the cryptate was recorded at 620 nm on a time-resolved fluorimeter (RUBYstar, BMG LABTECH, Champigny-sur-Marne, France) after excitation at 337 nm by a nitrogen laser, and the emission signal from the d2 was recorded at 682 nm on an Analyst reader (Molecular Devices) using a 640-nm excitation. The specific fluorescence signal was determined by subtracting the nonspecific signal in mock-transfected cells from the total fluorescence signal in the cells expressing the SNAP-tagged 5-HT$_6$R.

Statistical analysis

Statistical analyses were performed using Prism 4 (GraphPad Software Inc.). For two-sample and multiple comparisons (Western blots, cAMP production, and neurite length measurements), the unpaired Student's *t* test and one-way analysis of variance (ANOVA) followed by Newman-Keuls multiple comparisons test were used, respectively. Two-way ANOVA followed by Bonferroni's multiple comparisons test was used to evaluate significance of the Sholl analysis. $P < 0.05$ was considered to be statistically significant. Correlation between neurite length and the extent of 5-HT$_6$R constitutive activity in NG108-15 cells was evaluated 24 and 48 hours after transfection by linear regression analysis.

SUPPLEMENTARY MATERIALS

stke.sciencemag.org/cgi/content/full/13/618/eaax9520/DC1

Fig. S1. 5-HT$_6$R and GPRIN1 are colocalized at the soma plasma membrane of striatal and cortical neurons, but not in primary cilia.

Fig. S2. Analysis of cell lysates used for immunoprecipitation experiments.

Fig. S3. Effect of the phosphorylation of 5-HT$_6$R Ser^{350} on its interaction with GPRIN1 and neurite morphology.

Fig. S4. Effect of GPRIN1 coexpression with the 5-HT$_6$R on receptor cell surface expression in NG108-15 cells.

Fig. S5. GPRIN1 selectively affects the late stage of neurite growth in NG108-15 cells.

Fig. S6. The interaction between endogenous 5-HT$_6$R and GPRIN1 promotes neurite extension through a cAMP-dependent mechanism in striatal neurons.

View/request a protocol for this paper from *Bio-protocol*.

REFERENCES AND NOTES

1. S. K. Shenoy, R. J. Lefkowitz, Seven-transmembrane receptor signaling through β-arrestin. *Sci. STKE* **2005**, cm10 (2005).
2. J. Bockaert, L. Fagni, A. Dumuis, P. Marin, GPCR interacting proteins (GIP). *Pharmacol. Ther.* **103**, 203–221 (2004).
3. J. Bockaert, J. Perroy, C. Bécamel, P. Marin, L. Fagni, GPCR interacting proteins (GIPs) in the nervous system: Roles in physiology and pathologies. *Annu. Rev. Pharmacol. Toxicol.* **50**, 89–109 (2010).
4. A. C. Magalhaes, H. Dunn, S. S. G. Ferguson, Regulation of GPCR activity, trafficking and localization by GPCR-interacting proteins. *Br. J. Pharmacol.* **165**, 1717–1736 (2012).
5. S. L. Ritter, R. A. Hall, Fine-tuning of GPCR activity by receptor-interacting proteins. *Nat. Rev. Mol. Cell Biol.* **10**, 819–830 (2009).
6. J. Bockaert, P. Marin, A. Dumuis, L. Fagni, The 'magic tail' of G protein-coupled receptors: An anchorage for functional protein networks. *FEBS Lett.* **546**, 65–72 (2003).
7. J. Bockaert, G. Roussignol, C. Becamel, S. Gavarini, L. Joubert, A. Dumuis, L. Fagni, P. Marin, GPCR-interacting proteins (GIPs): Nature and functions. *Biochem. Soc. Trans.* **32**, 851–855 (2004).
8. C. Gérard, M.-P. Martres, K. Lefevre, M.-C. Miquel, D. Vergé, L. Lanfumey, E. Doucet, M. Hamon, S. El Mestikawy, Immuno-localization of serotonin 5-HT$_6$ receptor-like material in the rat central nervous system. *Brain Res.* **746**, 207–219 (1997).
9. L. Helboe, J. Egebjerg, I. E. M. de Jong, Distribution of serotonin receptor 5-HT$_6$ mRNA in rat neuronal subpopulations: A double in situ hybridization study. *Neuroscience* **310**, 442–454 (2015).
10. A. M. Kinsey, A. Wainwright, R. Heavens, D. J. S. Sirinathsinghji, K. R. Oliver, Distribution of 5-ht$_{5A}$, 5-ht$_{5B}$, 5-ht$_6$ and 5-HT$_7$ receptor mRNAs in the rat brain. *Brain Res. Mol. Brain Res.* **88**, 194–198 (2001).
11. F. J. Monsma Jr., Y. Shen, R. P. Ward, M. W. Hamblin, D. R. Sibley, Cloning and expression of a novel serotonin receptor with high affinity for tricyclic psychotropic drugs. *Mol. Pharmacol.* **43**, 320–327 (1993).
12. M. Ruat, E. Traiffort, J. M. Arrang, J. Tardivel-Lacombe, J. Diaz, R. Leurs, J. C. Schwartz, A novel rat serotonin (5-HT$_6$) receptor: Molecular cloning, localization and stimulation of cAMP accumulation. *Biochem. Biophys. Res. Commun.* **193**, 268–276 (1993).
13. X. Codony, J. M. Vela, M. J. Ramírez, 5-HT$_6$ receptor and cognition. *Curr. Opin. Pharmacol.* **11**, 94–100 (2011).

14. G. Maher-Edwards, R. Dixon, J. Hunter, M. Gold, G. Hopton, G. Jacobs, J. Hunter, P. Williams, SB-742457 and donepezil in Alzheimer disease: A randomized, placebo-controlled study. *Int. J. Geriatr. Psychiatry* **26**, 536–544 (2011).
15. G. Maher-Edwards, C. Watson, J. Ascher, C. Barnett, D. Boswell, J. Davies, M. Fernandez, A. Kurz, O. Zanetti, B. Safirstein, J. P. Schronen, M. Zvartau-Hind, M. Gold, Two randomized controlled trials of SB742457 in mild-to-moderate Alzheimer's disease. *Alzheimers Dement.* **1**, 23–36 (2015).
16. G. Maher-Edwards, M. Zvartau-Hind, A. J. Hunter, M. Gold, G. Hopton, G. Jacobs, M. Davy, P. Williams, Double-blind, controlled phase II study of a 5-HT_6 receptor antagonist, SB-742457, in Alzheimer's disease. *Curr. Alzheimer Res.* **7**, 374–385 (2010).
17. D. Wilkinson, K. Windfeld, E. Colding-Jørgensen, Safety and efficacy of idalopirdine, a 5-HT_6 receptor antagonist, in patients with moderate Alzheimer's disease (LADDER): A randomised, double-blind, placebo-controlled phase 2 trial. *Lancet Neurol.* **13**, 1092–1099 (2014).
18. A. Atri, L. Frölich, C. Ballard, P. N. Tariot, J. L. Molinuevo, N. Boneva, K. Windfeld, L. L. Raket, J. L. Cummings, Effect of idalopirdine as adjunct to cholinesterase inhibitors on change in cognition in patients with Alzheimer disease: Three randomized clinical trials. *JAMA* **319**, 130–142 (2018).
19. M. Jacobshagen, M. Niquille, S. Chaumont-Dubel, P. Marin, A. Dayer, The serotonin 6 receptor controls neuronal migration during corticogenesis via a ligand-independent Cdk5-dependent mechanism. *Development* **141**, 3370–3377 (2014).
20. F. Duhr, P. Déléris, F. Raynaud, M. Séveno, S. Morisset-Lopez, C. Mannoury la Cour, M. J. Millan, J. Bockaert, P. Marin, S. Chaumont-Dubel, Cdk5 induces constitutive activation of 5-HT_6 receptors to promote neurite growth. *Nat. Chem. Biol.* **10**, 590–597 (2014).
21. O. Riccio, G. Potter, C. Walzer, P. Vallet, G. Szabó, L. Vutskits, J. Z. Kiss, A. G. Dayer, Excess of serotonin affects embryonic interneuron migration through activation of the serotonin receptor 6. *Mol. Psychiatry* **14**, 280–290 (2009).
22. C. M. Ha, D. Park, Y. Kim, M. Na, S. Panda, S. Won, H. Kim, H. Ryu, Z. Y. Park, M. M. Rasenick, S. Chang, SNX14 is a bifunctional negative regulator for neuronal 5-HT_6 receptor signaling. *J. Cell Sci.* **128**, 1848–1861 (2015).
23. S.-H. Kim, D. H. Kim, K. H. Lee, S.-K. Im, E.-M. Hur, K. C. Chung, H. Rhim, Direct interaction and functional coupling between human 5-HT_6 receptor and the light chain 1 subunit of the microtubule-associated protein 1B (MAP1B-LC1). *PLOS ONE* **9**, e91402 (2014).
24. S.-H. Kim, M. Seo, H. Hwang, D.-M. Moon, G. H. Son, K. Kim, H. Rhim, Physical and functional interaction between 5-HT_6 receptor and Nova-1. *Exp. Neurobiol.* **28**, 17–29 (2019).
25. J. Meffre, S. Chaumont-Dubel, C. Mannoury la Cour, F. Loiseau, D. J. G. Watson, A. Dekeyne, M. Seveno, J. M. Rivet, F. Gaven, P. Déléris, D. Herve, K. C. F. Fone, J. Bockaert, M. J. Millan, P. Marin, 5-HT_6 receptor recruitment of mTOR as a mechanism for perturbed cognition in schizophrenia. *EMBO Mol. Med.* **4**, 1043–1056 (2012).
26. H.-M. Yun, J.-H. Baik, I. Kang, C. Jin, H. Rhim, Physical interaction of Jab1 with human serotonin 6 G-protein-coupled receptor and their possible roles in cell survival. *J. Biol. Chem.* **285**, 10016–10029 (2010).
27. H. M. Yun, S. Kim, H. J. Kim, E. Kostenis, J. I. Kim, J. Y. Seong, J. H. Baik, H. Rhim, The novel cellular mechanism of human 5-HT_6 receptor through an interaction with Fyn. *J. Biol. Chem.* **282**, 5496–5505 (2007).
28. R. Kohen, L. A. Fashingbauer, D. E. A. Heidmann, C. R. Guthrie, M. W. Hamblin, Cloning of the mouse 5-HT_6 serotonin receptor and mutagenesis studies of the third cytoplasmic loop. *Brain Res. Mol. Brain Res.* **90**, 110–117 (2001).
29. W. Deraredj Nadim, S. Chaumont-Dubel, F. Madouri, L. Cobret, M.-L. De Tauzia, P. Zajdel, H. Bénédetti, P. Marin, S. Morisset-Lopez, Physical interaction between neurofibromin and serotonin 5-HT_6 receptor promotes receptor constitutive activity. *Proc. Natl. Acad. Sci. U.S.A.* **113**, 12310–12315 (2016).
30. N. Iida, T. Kozasa, Identification and biochemical analysis of GRIN1 and GRIN2. *Methods Enzymol.* **390**, 475–483 (2004).
31. X. Ge, Y. Qiu, H. H. Loh, P.-Y. Law, GRIN1 regulates μ-opioid receptor activities by tethering the receptor and G protein in the lipid raft. *J. Biol. Chem.* **284**, 36521–36534 (2009).
32. J. C. Nordman, N. Kabbani, An interaction between α7 nicotinic receptors and a G-protein pathway complex regulates neurite growth in neural cells. *J. Cell Sci.* **125**, 5502–5513 (2012).
33. J. C. Nordman, W. S. Phillips, N. Kodama, S. G. Clark, C. A. Del Negro, N. Kabbani, Axon targeting of the alpha 7 nicotinic receptor in developing hippocampal neurons by Gprin1 regulates growth. *J. Neurochem.* **129**, 649–662 (2014).
34. I. Masuho, Y. Mototani, Y. Sahara, J. Asami, S. Nakamura, T. Kozasa, T. Inoue, Dynamic expression patterns of G protein-regulated inducer of neurite outgrowth 1 (GRIN1) and its colocalization with Gαo implicate significant roles of Gαo-GRIN1 signaling in nervous system. *Dev. Dyn.* **237**, 2415–2429 (2008).
35. H. Nakata, T. Kozasa, Functional characterization of Gαo signaling through G protein-regulated inducer of neurite outgrowth 1. *Mol. Pharmacol.* **67**, 695–702 (2005).
36. M. Brodsky, A. J. Lesiak, A. Croicu, N. Cohenca, J. M. Sullivan, J. F. Neumaier, 5-HT_6 receptor blockade regulates primary cilia morphology in striatal neurons. *Brain Res.* **1660**, 10–19 (2017).
37. M. Hamon, E. Doucet, K. Lefèvre, M.-C. Miquel, L. Lanfumey, R. Insausti, D. Frechilla, J. Del Rio, D. Vergé, Antibodies and antisense oligonucleotide for probing the distribution and putative functions of central 5-HT_6 receptors. *Neuropsychopharmacology* **21**, 68–76 (1999).
38. L. Hu, B. Wang, Y. Zhang, Serotonin 5-HT6 receptors affect cognition in a mouse model of Alzheimer's disease by regulating cilia function. *Alzheimer's Res. Ther.* **9**, 76 (2017).
39. A. J. Lesiak, M. Brodsky, N. Cohenca, A. G. Croicu, J. F. Neumaier, Restoration of physiological expression of 5-HT_6 receptor into the primary cilia of null mutant neurons lengthens both primary cilia and dendrites. *Mol. Pharmacol.* **94**, 731–742 (2018).
40. J. Zhang, C.-P. Shen, J. C. Xiao, T. J. Lanza, L. S. Lin, B. E. Francis, T. M. Fong, R. Z. Chen, Effects of mutations at conserved TM II residues on ligand binding and activation of mouse 5-HT_6 receptor. *Eur. J. Pharmacol.* **534**, 77–82 (2006).
41. L. I. Jiang, J. Collins, R. Davis, K.-M. Lin, D. DeCamp, T. Roach, R. Hsueh, R. A. Rebres, E. M. Ross, R. Taussig, I. Fraser, P. C. Sternweis, Use of a cAMP BRET sensor to characterize a novel regulation of cAMP by the sphingosine 1-phosphate/G_{13} pathway. *J. Biol. Chem.* **282**, 10576–10584 (2007).
42. L. P. Pellissier, J. Sallander, M. Campillo, F. Gaven, E. Queffeulou, M. Pillot, A. Dumuis, S. Claeysen, J. Bockaert, L. Pardo, Conformational toggle switches implicated in basal constitutive and agonist-induced activated states of 5-hydroxytryptamine-4 receptors. *Mol. Pharmacol.* **75**, 982–990 (2009).
43. A. G. Dayer, M. Jacobshagen, S. Chaumont-Dubel, P. Marin, 5-HT_6 receptor: A new player controlling the development of neural circuits. *ACS Chem. Nerosci.* **6**, 951–960 (2015).
44. L. T. Chen, A. G. Gilman, T. Kozasa, A candidate target for G protein action in brain. *J. Biol. Chem.* **274**, 26931–26938 (1999).
45. B. D. Semple, K. Blomgren, K. Gimlin, D. M. Ferriero, L. J. Noble-Haeusslein, Brain development in rodents and humans: Identifying benchmarks of maturation and vulnerability to injury across species. *Prog. Neurobiol.* **106–107**, 1–16 (2013).
46. N. F. Berbari, A. D. Johnson, J. S. Lewis, C. C. Askwith, K. Mykytyn, Identification of ciliary localization sequences within the third intracellular loop of G protein-coupled receptors. *Mol. Biol. Cell* **19**, 1540–1547 (2008).
47. F. Ango, L. Prézeau, T. Muller, J. C. Tu, B. Xiao, P. F. Worley, J. P. Pin, J. Bockaert, L. Fagni, Agonist-independent activation of metabotropic glutamate receptors by the intracellular protein Homer. *Nature* **411**, 962–965 (2001).
48. A. A. J. Rouault, L. K. Rosselli-Murai, C. C. Hernandez, L. E. Gimenez, G. G. Tall, J. A. Sebag, The GPCR accessory protein MRAP2 regulates both biased signaling and constitutive activity of the ghrelin receptor GHSR1a. *Sci. Signal.* **13**, eaax4569 (2020).
49. J.-Z. Yu, R. H. Dave, J. A. Allen, T. Sarma, M. M. Rasenick, Cytosolic $G\alpha_s$ acts as an intracellular messenger to increase microtubule dynamics and promote neurite outgrowth. *J. Biol. Chem.* **284**, 10462–10472 (2009).
50. Veeranna, K. T. Shetty, W. T. Link, H. Jaffe, J. Wang, H. C. Pant, Neuronal cyclin-dependent kinase-5 phosphorylation sites in neurofilament protein (NF-H) are dephosphorylated by protein phosphatase 2A. *J. Neurochem.* **64**, 2681–2690 (1995).
51. J.-H. Ahn, T. McAvoy, S. V. Rakhilin, A. Nishi, P. Greengard, A. C. Nairn, Protein kinase A activates protein phosphatase 2A by phosphorylation of the B56δ subunit. *Proc. Natl. Acad. Sci. U.S.A.* **104**, 2979–2984 (2007).
52. C. Savoia, J. B. Pujol, A. Vaucher, U. De Marchi, C. Rieker, E. Heikkilä, A. Núñez Galindo, L. Dayon, E. Dioum, GPRIN1 modulates neuronal signal transduction and affects mouse-learning behavior. *bioRxiv* **2018**, 291377 (2018).
53. S. Claeysen, P. Faye, M. Sebben, S. Lemaire, J. Bockaert, A. Dumuis, Cloning and expression of human 5-HT4S receptors. Effect of receptor density on their coupling to adenylyl cyclase. *Neuroreport* **8**, 3189–3196 (1997).
54. D. Maurel, L. Comps-Agrar, C. Brock, M.-L. Rives, E. Bourrier, M. A. Ayoub, H. Bazin, N. Tinel, T. Durroux, L. Prezeau, E. Trinquet, J.-P. Pin, Cell-surface protein-protein interaction analysis with time-resolved FRET and snap-tag technologies: Application to GPCR oligomerization. *Nat. Methods* **5**, 561–567 (2008).

Acknowledgments: Mass spectrometry analyses were performed using the facilities of the Functional Proteomics Platform of Montpellier, Languedoc-Roussillon. Confocal microscopy was performed using the facilities of the Montpellier Imaging Resources (MRI) platform. The BRET and FRET experiments were performed using the ARPEGE (Pharmacology, Screening, Interactome) platform facility (IGF, Montpellier, France). We thank Q. Durix and E. Belan from the iExplore animal facility, RAM, Biocampus. We also thank A. Monteil and C. Lemmers from the virus production facility, PVM (Biocampus Montpellier, CNRS UMS 3426) for the production of viral particles. We thank M. Asari for help with iconography. We also thank S. Morisset for the gift of the 5-HT_6R–GFP plasmid. **Funding:** This work was supported by grants from the ANR [Sero6Cognet (ANR-11-BSV4-008-01) and Sero6Dev (ANR-17-CE16-0010-01)], CNRS, INSERM,

and the University of Montpellier and la Région Occitanie. We also thank the Foundation for Medical Research (FRM). **Author contributions:** P.M., J.B., and S.C.-D. designed the experiments. M.S. performed mass spectrometry experiments. C.N.P. and L.R. studied neurite growth and branching in culture. C.N.P. performed BRET, FRET, and biochemistry experiments. V.D. performed immunohistochemistry experiments. S.C.-D. performed BRET and pharmacology experiments. P.M., J.B., and S.C.-D. wrote the manuscript. **Competing interests:** The authors declare that they have no competing interests. **Data and materials availability:** All data needed to evaluate the conclusions in the paper are present in the paper or the Supplementary Materials.

Submitted 7 May 2019
Accepted 28 January 2020
Published 11 February 2020
10.1126/scisignal.aax9520

Citation: C. N. Pujol, V. Dupuy, M. Séveno, L. Runtz, J. Bockaert, P. Marin, S. Chaumont-Dubel, Dynamic interactions of the 5-HT_6 receptor with protein partners control dendritic tree morphogenesis. *Sci. Signal.* **13**, eaax9520 (2020).

Dynamic interactions of the 5-HT$_6$ receptor with protein partners control dendritic tree morphogenesis

Camille N. Pujol, Vincent Dupuy, Martial Séveno, Leonie Runtz, Joël Bockaert, Philippe Marin and Séverine Chaumont-Dubel

Sci. Signal. **13** (618), eaax9520.
DOI: 10.1126/scisignal.aax9520

Taking the time to signal

The serotonin receptor 5-HT$_6$R is a GPCR exclusively found in the nervous system that has emerged as a potential therapeutic target in various neurological disorders. Although preliminary studies suggested that 5-HT $_6$R antagonists have procognitive effects, clinical trials have been disappointing. Pujol *et al.* analyzed the dynamics of 5-HT$_6$ R interactions with other proteins and found that after its previously characterized interaction with and phosphorylation by the kinase Cdk5, the 5-HT $_6$R interacted with GPRIN1, a promoter of neurite extension. These sequential interactions enhanced 5-HT $_6$R constitutive activity, promoting neurite extension and branching in neuroblastoma cells and primary striatal neurons. The GPRIN1–5-HT$_6$R interaction was reduced by 5-HT$_6$R antagonist, suggesting that the dynamic interactions of this receptor are regulated by its conformational state.